

Assessing the role of exogenous NO on plants and microbial communities in soil

Eduardo Pérez-Valera                                          <img alt="ORCID

in complex environments, such as soil and plant-soil systems, remains unexplored due to methodological constraints in both dynamically manipulating and measuring trace gas fluxes [16].

In plants, NO is also a key signaling molecule activating defense mechanisms following pathogen attack [17]. Its effectiveness in protecting plants against microbial pathogens as an antimicrobial agent, due to its toxic effects, depends however on its concentration and the plant's physiological conditions—whether under stress or not [18]. At low concentrations, NO can also influence seed germination, root development, stomatal closure, and adaptive responses to biotic and abiotic stresses, whereas excessive levels suppress leaf expansion [19–23]. Although NO is central to several physiological and biochemical processes in plants, little is known about the ability of plants to perceive exogenous NO and its consequence for plant physiology. Studies based on the exposure of plant tissues to chemical NO donors or of the aerial part of plants to gaseous NO have shown that such treatments modulate the expression of numerous genes, promote NO-dependent post-translational protein modifications, and affect plant morphological traits and physiological processes [24]. Yet, the relevance of NO concentrations typically found in the soil atmosphere for plant physiology, growth and plant-microbe interactions remains unclear. This is partly due to the lack of reliable experimental systems that enable the precise manipulation and quantification of trace gas concentrations, such as NO, in soil.

Here, we investigated the extent to which exogenous NO may affect directly or indirectly plant physiology and growth as well as soil and plant-associated microbial communities, with a focus on C and N cycling processes in soil. For this purpose, we used a newly developed innovative plant-soil mesocosm system that dynamically changes background NO concentrations while also allowing the soil-atmosphere exchange of other trace gases to be measured [25]. *Arabidopsis* and tomato plants were grown under 0 ppbv or 400 ppbv NO for 5 weeks before analyzing the bacterial and fungal communities in soil, rhizosphere and roots, plant physiological status, N balance as well as CO₂, N₂O and NO fluxes. We hypothesized that (i) due to its antimicrobial properties, exogenous NO would detrimentally affect the abundance and diversity of microbial communities, (ii) N-cycling microbial communities would particularly be affected, as NO can also act both as a substrate and a regulatory molecule, (iii) root-associated microbes would be more susceptible due to direct and indirect effects mediated by exogenous NO-induced physiological and morphological changes in *Arabidopsis* and tomato plants.

Materials and methods

Plant and soil materials, plant germination, and mesocosm preparation

The soil was collected at the CEREEP research station, France (N 48°17'14.48", E 2°40'34.64"). The soil is classified as sandy loam (clay: 6.9%; silt: 19.0%; sand: 74.1%) with a C/N ratio of 12.25 and a pH (H₂O) of 5.22. Soil mesocosms were prepared by filling cylindrical Plexiglas cuvettes (126.5 mm diameter, 200 mm height) with 1633 g of sieved and homogenized soil corresponding to a depth of 10 cm [25]. Water was added to reach 20% WFPS on the first day, and then, after the transfer of the seedlings, it was maintained at 40% WFPS throughout the experiment.

Arabidopsis and tomato seeds were first surface-sterilized with 70% ethanol (1 min) and 6% sodium hypochlorite (10 min) and then rinsed five times with sterile distilled water. Two independent experiments were carried out by sowing either three *A. thaliana* Col-0 (WT) or three tomato *S. lycopersicum* (Moneymaker) seedlings per mesocosm.

Automated plant-soil mesocosm system and flux measurements

Twelve mesocosms per plant species were incubated for 37 days at 20°C in the automated plant-soil mesocosm system (AU-MES) designed for controlled headspace and soil flushing with nitric oxide (NO), as detailed in [25]. Briefly, these mesocosms have an integrated LED lighting system in the upper lid for optimum plant growth with a 10-h light cycle and a soil flushing inlet at the bottom lid to ensure even soil flushing. Six mesocosms were soil-flushed with NO at 400 ppbv (NO₄₀₀) on specific days (7–11, 16–18, 23–26, and 32–35), while the remaining six were soil-flushed the same days with ambient air (NO₀) and served as controls (Fig. S1). On day 13, all mesocosms were fertilized with (15NH₄)₂SO₄ at a 30% and 70% atom enrichment for the *Arabidopsis* and tomato experiments, respectively, and applied at a rate of 60 kg N ha⁻¹. A NO concentration of 400 ppbv was selected as representative of the range of values reported in a previous year-long study, in which monthly averages of up to 400 ppbv were observed in rainforest soils [8]. This concentration is also consistent with NO levels of up to 460 ppbv measured at a tropical forest site during a one-month monitoring period [9].

The gas fluxes from the mesocosms were routed through multiposition valves to a multigas analyzer, enabling continuous monitoring of trace gas concentrations (CO₂, N₂O, and NO) via mid-infrared laser spectrometry. Measurements followed a 144-min sampling sequence, with each mesocosm (outlet) and the reference chamber (inlet) being measured for 6 min across the 12 mesocosms. The system operated in two modes: NO soil flushing mode and headspace gas flux measurement mode (Fig. S1). Throughout the incubation, alternating periods of soil NO flushing and trace gas flux measurements were conducted.

Sampling of the mesocosms

After 37 days, soil samples (hereinafter referred to as "bulk soil") were collected in triplicate from each mesocosm. Soil samples were collected and separated into two depths (0–5 cm and 5–10 cm), taking into account the potential effects of moistening and ¹⁵N fertilization, which was applied to the top layer. The samples were then pooled and homogenized by layer for each mesocosm, resulting in six replicates per depth and NO concentration. To collect the rhizospheric soil, the loose soil was first gently removed by kneading and shaking the roots. The roots from all three plants within each mesocosm were combined in a clean, sterile 15 ml Falcon tube containing 2.5 ml phosphate buffer (per liter: 6.33 g of NaH₂PO₄, 16.5 g of Na₂HPO₄, 200 µl Silwet L-77). The rhizospheric soil was separated from the roots by vortexing at maximum speed for 15 s at 3200 × g. Most of the supernatant was removed and the remaining loose pellets were resuspended and transferred to a 1.5 ml tube, then centrifuged for 5 min at 10 000 × g. The resulting pellet was designated as the rhizosphere compartment. For the endophytic compartment, the cleaned roots from the previous vortexing step were transferred to another 15 ml Falcon tube containing 2.5 ml phosphate buffer and sonicated for less than 5 min to avoid overheating. After removing the buffer, sonicated roots were defined as the endophytic compartment. All bulk soil, rhizosphere, and root endophytic samples were transferred into 2 ml tubes and stored at -80°C.

Plant RNA extraction and RT-qPCR relative gene expression

RNA samples were isolated from one frozen leaf, first tissue was ground with a potter pestle, and RNA was extracted using the SV

Total RNA isolation system as per the manufacturer's guidelines (Promega). The quality of the RNA was verified prior to reverse transcription with High-Capacity cDNA Reverse Transcriptase Kit (Applied Biosystems). Reverse transcription quantitative PCR was carried out following the protocol provided by the manufacturer using a Go-Taq qPCR master mix kit (Promega). Cq and primer efficiency for each well were obtained using LinReg software. Gene expression level was then calculated following the method described by Ganger et al. [26]. The $\Delta\Delta Cq$ values were used for statistical analyses, and the relative gene expression ($10^{-\Delta\Delta Cq}$) was plotted. We quantified the gene expression involved in iron homeostasis, defense-growth balance and nitrogen metabolism in *Arabidopsis* and tomato plants (Table S1). Gene expression levels were normalized to two reference genes for *Arabidopsis*—At4g26410 and AtPTB— [27] and three reference genes for tomato—SlActin [28], SlTIP41 and Slg025390.2 [29]. The reverse transcription reactions were done with technical duplicates using the primers detailed in Table S2.

Plant traits

To avoid stressing plants for biochemical analyses, the leaf area (in cm^2) was quantified using images of the mesocosms taken from above on day 37 (sampling day). Plants showing severe growth limitations were excluded from the analysis. In the case of the tomato experiment, it was not possible to quantify the leaf area due to the overlapping leaves. Only tomato plants were used for biomass and ^{15}N analyses, as the limited plant material available for *Arabidopsis* prevented further analyses.

Assessment of microbial community composition and diversity

DNA was extracted from bulk soil (2 NO treatments \times 2 soil depths \times 6 replicates) as well as rhizospheric soil samples (2 NO treatments \times 6 replicates) from both *Arabidopsis* and tomato using the DNeasy PowerSoil-htp 96 well DNA isolation kit (Qiagen, France). For the root samples (2 NO treatments \times 6 replicates), the DNA was extracted using the DNeasy Plant kit (Qiagen, France) according to the manufacturer's instructions. Extracted DNA was quantified using the Quant-IT dsDNA HS Assay Kit (Invitrogen, Carlsbad, CA, USA). The V3-V4 16S rRNA gene region was amplified using a 2-step PCR as described in [30]. PCR products were verified on a 2% agarose gel and normalized using the SequalPrep Normalisation plate kit (Invitrogen, Carlsbad, CA, USA). Sequencing was performed on an Illumina MiSeq (2 \times 250 bp) using the MiSeq Reagent Kit v2.

Demultiplexing and trimming of Illumina adaptors and barcodes were performed using Illumina MiSeq Reporter software (version 2.5.1.3). Sequence data for both 16S rRNA and ITS were analyzed using an in-house Python pipeline (available upon request), as described in [30]. Briefly, paired-end sequences were merged, and short sequences (<400 bp for 16S and <300 bp for ITS) and those identified as chimeras removed. OTU identity thresholds were set at 94% for 16S and 97% for ITS. Taxonomy was assigned using UCLUST (USEARCH v11) [31] and the SILVA database (v138.1/2020) [32] for 16S rRNA and using BLAST [33] and the UNITE reference database (v8.3/2021) [34] for ITS. Sequences from the 16S rRNA gene that were classified as mitochondria or chloroplast were excluded. A total of 8163 OTUs ($50\,713 \pm 20\,039$ (mean \pm SD) reads per sample) and 6292 OTUs ($59\,946 \pm 7774$ reads per sample) were generated for the 16S rRNA and ITS, respectively.

Quantification of total bacterial, ammonia-oxidizing and denitrifier communities

Real-time quantitative PCR assays were used to determine the abundances of total bacterial, fungal, ammonia-oxidizing and denitrifying communities in both bulk soil and rhizosphere samples only, due to low DNA yields from the root samples. Total bacterial community and fungal abundances were quantified using 16S rRNA and ITS primers previously described [35]. Ammonia-oxidizing archaeal (AOA), bacterial (AOB) and comammox communities were quantified as in [36]. Denitrifying communities carrying the *nirK* and *nirS* genes were assessed as in [30] and *nosZI* and *nosZII* genes as in [37]. Negative controls were included in each measurement and inhibition tests prior to qPCR were negative.

Soil and plant N-pool analyses

The ^{15}N balance was assessed in bulk soil samples from 0–5 cm and 5–10 cm depth, focusing on ^{15}N recovery in total nitrogen (TN), extractable organic and mineral N, and microbial biomass N (MBN). Homogenized samples (50 g) were extracted with 0.5 M K_2SO_4 (1:2, soil:solution) [38] and stored at -20°C . NH_4^+ and NO_3^- concentrations were measured by microplate spectrophotometry [39]. Total dissolved N (TDN) and dissolved organic carbon (DOC) were analyzed using a TOC/TN analyzer. Dissolved organic N (DON) was calculated as the difference between TDN and mineral N [40]. MBN was determined by chloroform fumigation extraction without a correction factor [39]. ^{15}N enrichment in NH_4^+ , NO_3^- , DON, and MBN was quantified by sequential diffusion in acid traps followed by elemental analysis-isotope ratio mass spectrometry (EA-IRMS) [40].

The tomato plants were separated into above-ground (leaves and shoots) and below-ground (roots) compartments. The roots were rinsed with tap water, and all plant samples were dried at 55°C until a constant weight was reached, then finely ground and stored in tin capsules over silica gel for ^{15}N analysis. In addition, ~ 10 g of soil from each depth was similarly processed to assess ^{15}N recovery. ^{15}N enrichment and total N concentrations in both plant sections and soil were quantified using EA-IRMS. Isotopic data and ^{15}N tracer recovery across plant and soil nitrogen pools were calculated using established formulas [40].

Statistical analysis

Statistical analyses were performed using R statistical software (version 4.2.2) [41]. Differences in plant gene expression and leaf area were evaluated using t-tests with log10-transformed data. Taxonomic bar plots from microbial communities were computed using microeco (v1.8.0) [42]. Alpha diversity (i.e. OTU richness and Shannon diversity index) was calculated after rarefaction (13 000 and 15 700 reads per sample without replacement for 16S rRNA and ITS, respectively). Samples under rarefaction limits were excluded. Principal Coordinates Analysis (PCoA) and permutational multivariate analysis of variance (PERMANOVA) were run using Bray–Curtis dissimilarity matrices. Beta diversity PCoA analyses were plotted using phyloseq v1.41.1 [43] using rarefied tables. PERMANOVAs were run on the rarefied matrices using the adonis2 function (999 permutations) in vegan v2.6–4 [44]. Pairwise differences in bacterial and fungal composition were analyzed using the pairwise.adonis function (999 permutations, corrected $P < .05$ using Benjamini–Hochberg) of the pairwiseAdonis v0.4.1 package [45]. In bulk soil samples, the effects of NO treatment, soil depth, and their interaction on alpha diversities, as well as on the abundance of bacteria, fungi, ammonia oxidizers, denitrifiers, and nitrogen pools, were assessed using ANOVA. Additionally, similar

ANOVAs were conducted across all sample types (bulk, rhizosphere, and root) to evaluate the effects of NO treatment, compartment, and their interaction. ANOVAs were run independently for *Arabidopsis* and tomato experiments. Pairwise differences in alpha diversity, microbial abundances and N pools were evaluated using non-parametric Kruskal-Wallis tests followed by Fisher's least significant difference with Benjamini-Hochberg correction ($P < .05$).

Flux data were preprocessed using a custom R-script, focusing on the complete time series and individual phases, with trace gas fluxes calculated only during headspace flushing periods [25]. T-tests ($P = .05$) were applied to evaluate NO effects on leaf area, soil-atmosphere trace gas fluxes and compare cumulative fluxes between control and NO-treated soils. Data visualization, including gas flux and nitrogen dynamics graphs, was conducted with OriginPro 2020b (OriginLab Corporation).

Results

Plant responses to NO_0 and NO_{400} treatments

Enrichment of the ambient air stream with NO at 400 ppbv in the automated plant-soil mesocosms had a limited impact on the transcript levels of plant genes related to N metabolism, defense mechanisms, hormone responses and growth (Fig. 1). Thus, only the transcripts levels of AtPAL1 and AtPDF1.2—involved in plant metabolism and/or the plant defensive response—were significantly affected by NO_{400} in *Arabidopsis*, showing an increase of 112% and a decrease of 89.56% compared to NO_0 , respectively. NO_{400} also led to a significantly larger leaf area in *Arabidopsis* plants, with an average increase of 61% compared to NO_0 (Fig. S2). A small but significant increase in the tomato belowground, but not aboveground, biomass was also observed in response to NO_{400} without any significant changes in the plant N-content (Table S3).

Taxonomic composition of bacterial and fungal communities in response to increased NO

Increased NO concentration in the soil atmosphere did not alter the relative abundance of the major bacterial or fungal phyla, regardless of the compartment or of the plant species (Fig. S3). The bacterial communities in bulk soil, both at 0–5 cm and 5–10 cm depth, and in the rhizosphere of *Arabidopsis* and tomato plants, were dominated by Firmicutes (35%–49% relative abundance), followed by Gammaproteobacteria (10%–15%), Actinobacteria (9%–13%) and Alphaproteobacteria (6%–10%) (Fig. S3A). At the genus level, *Bacillus* (11%–23%) and *Tumbelacillus* (2%–10%) dominated in bulk soil (Fig. S4A). The predominant bacterial groups in plant roots strongly differed from those in the rhizosphere or bulk soil, with Gammaproteobacteria—*Massilia* in *Arabidopsis* and *Pseudomonas* in tomato—dominating in the roots for both plant species, followed by Alphaproteobacteria and Bacteroidetes. In fungal communities, Ascomycota was the dominant phyla in the bulk soil at both depths and in the rhizosphere of tomato plants, with *Pseudeurotium* as the more abundant genus (Figs. S3B and S4B). Basidiomycota, mainly the genus *Sebacina*, dominated in *Arabidopsis* roots (>93%) whereas the composition of the fungal community was more even in tomato roots with similar proportions of Basidiomycota, Ascomycota, Olpidiomycota and Glomeromycota.

Effects of NO on microbial alpha diversity

Exogenous NO had no effect on the alpha diversity of the bacterial communities, whereas it significantly altered the fungal diversity (Shannon index) in the *Arabidopsis* experiment (Fig. 2).

A significant NO \times compartment interaction was also found for fungal richness in the *Arabidopsis* experiment (Fig. 2B, Table S4). Nevertheless, differences in the alpha diversity were more pronounced based on the soil depth, plant species and plant compartment. Thus, the bacterial and fungal OTU richness were primarily affected by the compartment, with decreases ranging between 54 and 58% in the roots compared to the other compartments, regardless of the plant species. Similarly, the Shannon index was the lowest in the roots but without significant differences with the bulk soil for fungi in tomato (Fig. 2C and D). For both bacterial and fungal communities, the rhizosphere effect was stronger in *Arabidopsis* than in tomato. Finally, the soil depth had a significant effect on the bacterial OTU richness and the Shannon index, with higher diversity in the bulk soil at 5–10 cm depth compared to 0–5 cm depth (Fig. 2A, C, Table S4).

Beta diversity of microbial communities

Next, we tested the effect of exogenous NO concentration on the beta diversity of bacterial and fungal communities using principal coordinate analysis (PCoA) and permutational multivariate analysis of variance (PERMANOVA) (Fig. 3, Table S5). In the *Arabidopsis* experiment, NO_{400} had a limited but significant impact on the specific composition of fungal communities in the bulk soil at both depths, as shown by the PERMANOVA (Fig. 3) and the pairwise PERMANOVAs (Table S5). Nevertheless, the primary drivers of both microbial communities were the compartment followed by soil depth (Fig. 3).

Abundance of total bacterial and fungal communities as well as of ammonia-oxidizers and denitrifiers

Quantification of ammonia-oxidizing and denitrifier community abundances by qPCR revealed that NO_{400} had a significant effect on ammonia oxidizers and denitrifiers only in the *Arabidopsis* experiment (Fig. 4, Table S4), with NO_{400} leading to a significant decrease in the abundance of ammonia-oxidizing AOB compared to NO_0 . A significant interaction was also observed between NO treatment and compartment (i.e. bulk soil or *Arabidopsis* rhizosphere) for the abundance of ammonia-oxidizing comammox clade B and *nirK*-denitrifiers. Ammonia-oxidizer and denitrifier abundances also varied significantly with soil depth, compartment and plant species. Total bacterial and fungal abundances were unaffected by NO in either species (Fig. S5, Table S4).

Emissions and cumulative fluxes of CO_2 , N_2O , and NO

Emissions of CO_2 , N_2O and NO gases were monitored throughout the 37-day incubations periods in all mesocosms during six treatment phases (i.e. seedling transfer, ^{15}N fertilization and 4 NO flushing periods; Figs. 5 and 6). Cumulative fluxes of CO_2 , N_2O and NO varied significantly with the experiment, the treatment phase, and the light cycle (Table 1). After phase 3 (2nd NO flushing) corresponding to the leaf emergence, the CO_2 emissions showed a clear pattern aligned with the light cycles, with higher emissions when the lighting was off than when it was on. In the *Arabidopsis* experiment, NO_{400} significantly reduced CO_2 emissions with lights on during phases 3 and 4, resulting in a significant decrease by 12% in cumulative CO_2 emissions (Table 1). On the contrary, with lights off, NO_{400} significantly increased CO_2 respiration during phases 2, 3 and 6. In the tomato experiment, similar effects of NO_{400} on CO_2 fluxes were observed with decreases with light on (phases 2 and 4) and increases with light off (phase 4).

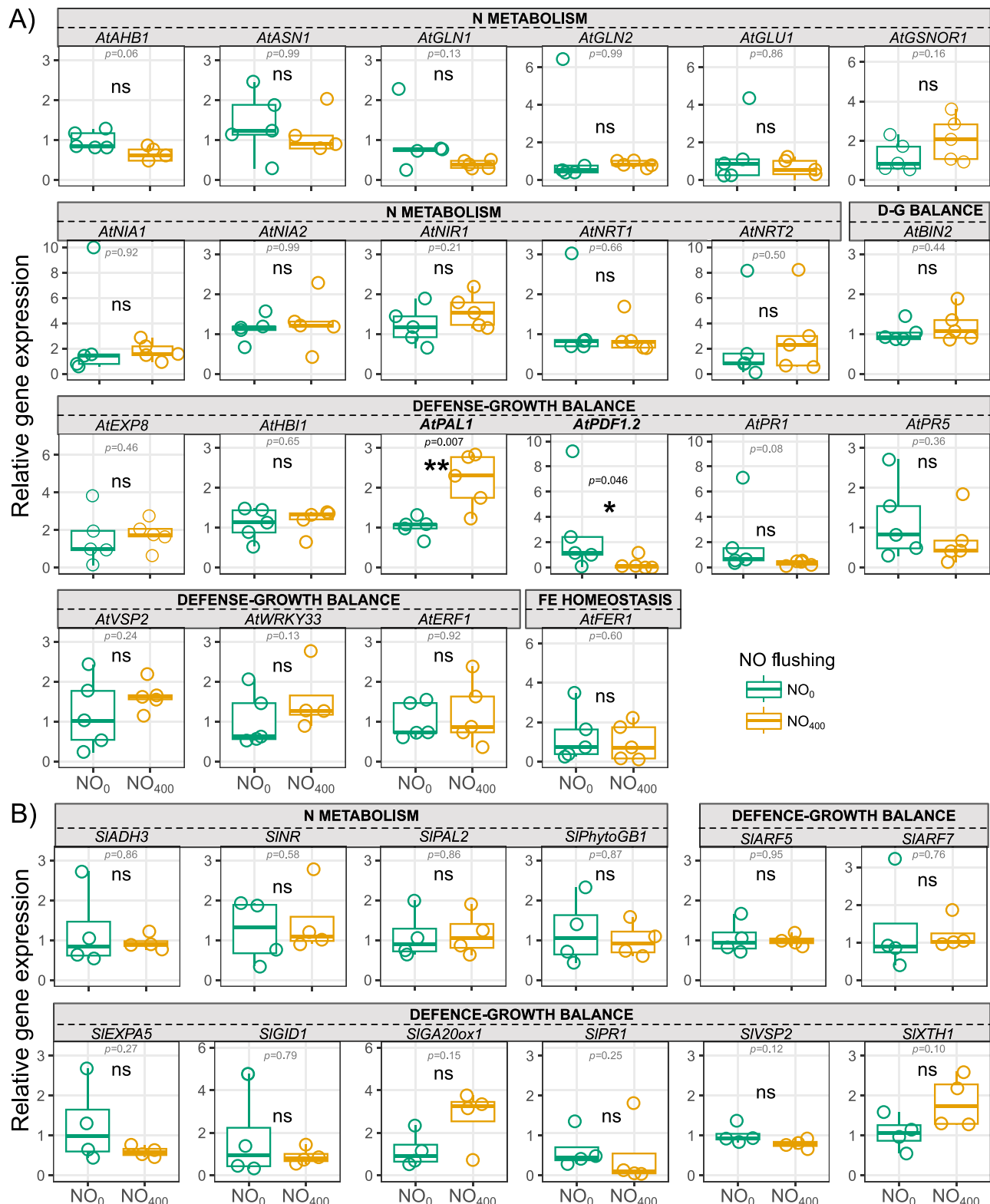


Figure 1. Relative expression of plant genes involved in N metabolism, defense-growth balance and iron homeostasis in the leaves of (A) Arabidopsis and (B) tomato plants subjected to NO treatments (NO₀ and NO₄₀₀). For each box, the central horizontal line represents the median; the lower and upper edges correspond to the first and third quartiles, respectively; whiskers extend to the minimum and maximum values no further than 1.5 times the interquartile range. Asterisks indicate statistical differences (t-tests: ns not significant).

The impact of NO₄₀₀ compared to NO₀ was more pronounced on N₂O emissions, particularly in the tomato experiment (Figs. 5 and 6). Thus, NO₄₀₀ reduced N₂O emissions by a total of 59% after the second NO flush (during phase 4) and by a total of 47% over the entire incubation period, regardless of light

conditions (Table 1). In the Arabidopsis experiment, NO₄₀₀ significantly decreased N₂O emissions only during phase 2 with lights on.

NO emissions were significantly affected by flushing with NO₄₀₀ only in the Arabidopsis experiment, increasing by 17 to

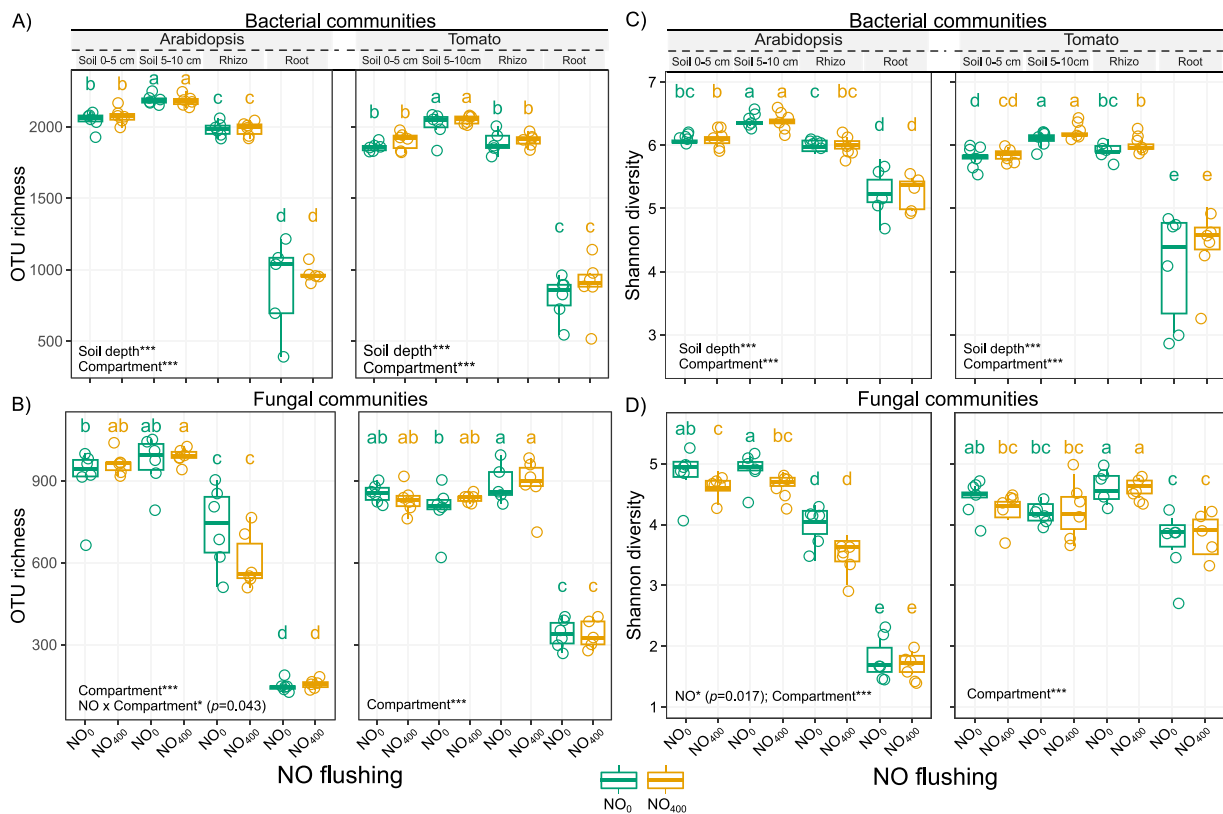


Figure 2. Boxplots showing the differences in the observed OTU richness of (A) bacterial and (B) fungal communities, and the Shannon diversity of (C) bacterial and (D) fungal communities in bulk soil, rhizosphere and root samples of Arabidopsis and tomato subjected to NO treatments (NO₀ and NO₄₀₀). For each box, the central horizontal line indicates the median, while the lower and upper edges represent the first and third quartiles, respectively. The whiskers extend to the minimum and maximum values, provided they do not exceed 1.5 times the interquartile range. Distinct letters above the boxes indicate significant differences based on non-parametric Kruskal-Wallis tests, followed by Fisher's least significant difference with Benjamini-Hochberg correction for pairwise comparisons ($P < .05$). Statistical significance for the effects of (i) NO, soil depth, and their interaction, and (ii) NO, compartment (bulk soil, rhizosphere and root), and their interaction, is indicated by asterisks in the figure (* $P < .05$, ** $P < .01$, *** $P < .001$), with ANOVA model outputs provided in Table S4.

19% when lights were off in phase 2 and 3, while decreasing by 14% after fertilization in phase 3 with lights on.

Nitrogen dynamics in response to exogenous NO

Exogenous NO significantly altered the ¹⁵N recovery of soil nitrogen forms compared to the 0 ppbv NO control, though the impact was limited and varied depending on the nitrogen form, the plant experiment, and the soil depth (Table 2). Thus, in the Arabidopsis experiment, NO₄₀₀ led to a significant decrease in total ¹⁵N recovery for NO₃⁻ while a higher recovery was observed for MBN but only at 0-5 cm. In the tomato experiment, NO₄₀₀ resulted in a decreased ¹⁵N recovery for both NO₃⁻ and total nitrogen (TN) at 0-5 cm and an increased ¹⁵N recovery at 5-10 cm for NO₃⁻ only. Overall, higher ¹⁵N recoveries were consistently observed in the upper soil layer (0-5 cm), compared to the lower layer (5-10 cm), as well as in the tomato aboveground biomass (~80%) compared to the belowground biomass (~5%). However, exogenous NO had no significant impact on the ¹⁵N recovery between aboveground and belowground biomass (Table S6). In the Arabidopsis experiment only, exogenous NO consistently lowered NH₄⁺ concentrations independent of soil depth, whereas NO₃⁻ exhibited variable responses (Fig. S6, Table S4).

Discussion

Fumigation of plants with NO has allowed the identification of numerous NO-responsive genes and S-nitrosated proteins

[46–50]. For example, this method shed light on the role of NO in regulating metabolism [51], nitrosoglutathione reductase activity [52] and salicylic acid (SA) biosynthesis [46]. Because NO can react with air to form NO₂ that can also trigger stress responses in plants, caution is needed when interpreting results especially from NO fumigation experiments performed in closed chambers [53]. However, NO₂ concentrations did not increase after NO flushing in the newly developed plant-soil mesocosm used in our study [25]. The NO concentration of 400 ppbv used in our experiment corresponds to natural soil fluxes [8, 9] and falls within the range reported for highly polluted urban environments (200–700 ppbv) [54].

We observed that the NO₄₀₀ treatment of Arabidopsis and tomato did not impact most of the tested transcripts encoded by N-metabolism-, defense-, growth- and iron uptake-related genes. Nevertheless, NO₄₀₀ significantly increased the expression of AtPAL1, while decreasing that of AtPDF1.2 encoding phenylalanine ammonia lyase 1 and the plant defensin 1-2, respectively. These results are in accordance with previous published data reporting that NO promotes AtPAL expression in Arabidopsis and tobacco [48, 55]. Regarding AtPDF1.2, this jasmonate (JA)-responsive gene was found to be regulated through NO-dependent processes in few studies. For instance, Huang et al. [46] observed an accumulation of AtPDF1.2 transcript in response to NO in plants impaired in SA biosynthesis, suggesting that SA acts as a negative regulator of the NO-dependent up-regulation of the corresponding gene. A NO-dependent induction of AtPDF1.2 expression was also found in Arabidopsis embryos

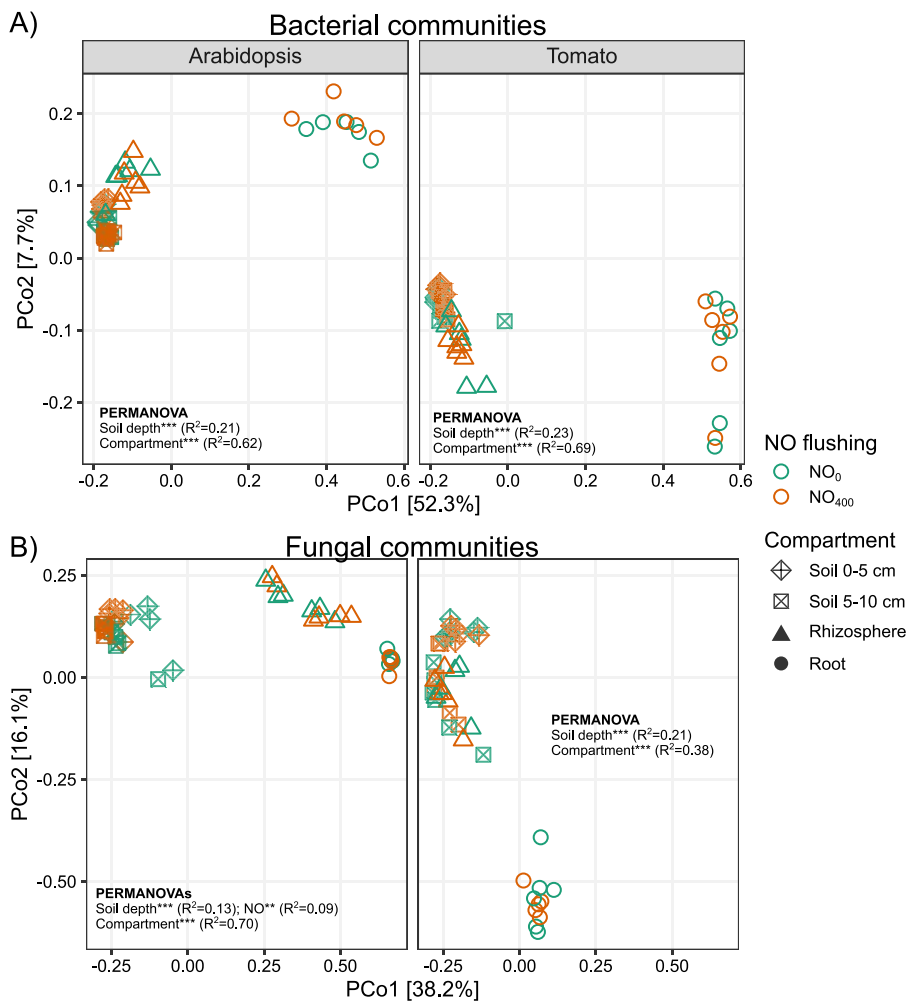


Figure 3. Principal Coordinate Analysis (PCoA) of Bray–Curtis dissimilarities of (A) bacterial communities and (B) fungal communities in bulk soil, rhizosphere and root samples of Arabidopsis and tomato subjected to NO treatments (NO₀ and NO₄₀₀). Two PERMANOVAs per plant species and microbial group were performed to assess (i) the effects of NO, soil depth, and their interaction by only including bulk soil samples, and (ii) the effects of NO, compartment (soil, rhizosphere, and root), and their interaction. Statistical significance levels are indicated by asterisks in the figure (* $P < .05$, ** $P < .01$, *** $P < .001$).

[56]. Authors of this study proposed a model in which NO promotes the synthesis of JA which, in turn, represses the expression of the transcription factor MYC2 involved in the down-regulation of AtPDF1.2 expression. More recently, Pescador *et al.* [57] demonstrated that in Arabidopsis plants pre-exposed to volatiles promoting induced systemic resistance, the induced expression of AtPDF1.2 triggered by the pathogenic fungus *Botrytis cinerea* was inhibited by the NO scavenger CPTIO suppressing NO accumulation. Overall, our results strongly suggest that Arabidopsis plants perceived, directly or indirectly, exogenous NO. This was supported by the significantly larger leaf area in plants exposed to NO₄₀₀. Similarly, exogenous NO has been shown to promote plant growth, including leaf expansion [58]. However, in our assays no physiological or biomass changes were observed in tomato leaves subjected to NO₄₀₀. Although no effects of elevated NO concentrations on the aboveground biomass of tomatoes were detected, it should be noted that the mesocosm incubation system only allowed for undisturbed plant development up to 25 days after germination due to space constraint. However, the tomato plants were still growing, as evidenced by the greater CO₂ consumption during the final phase. Since this space constraint affected both NO₀ and NO₄₀₀ treated plants (no significant NO

effect during phase 6), it cannot be considered a confounding factor and does not affect our conclusions. Nevertheless, our mesocosms provide a significant advance in the study of the role of NO on processes in the plant–soil systems. Future experiments using mesocosms optimized for plant development are needed to support and extend our results.

As previously reported [59, 60], we found that microbial communities were mostly influenced by the plant compartment, with the lowest alpha diversity in the root tissues, regardless of the plant species. The plant compartment also contributed up to 69% and 70% of the variation in the structure of the bacterial and fungal communities, respectively. Changes in microbial communities from soil to the endosphere were attributed to both abiotic and biotic filtering, driven by significant differences in nutrient availability, oxygen levels, and pH between soils and roots, as well as the selective recruitment of microorganisms by plants [60–62]. The enrichment of Proteobacteria in Arabidopsis and tomato roots is consistent with previous studies, although this plant effect can be modulated by soil type and plant genotype [63–67]. In line with the inability of Arabidopsis to establish a functional arbuscular mycorrhizal symbiosis [68], we observed the specific recruitment of Glomerales in tomato roots only. Glomerales include arbuscular

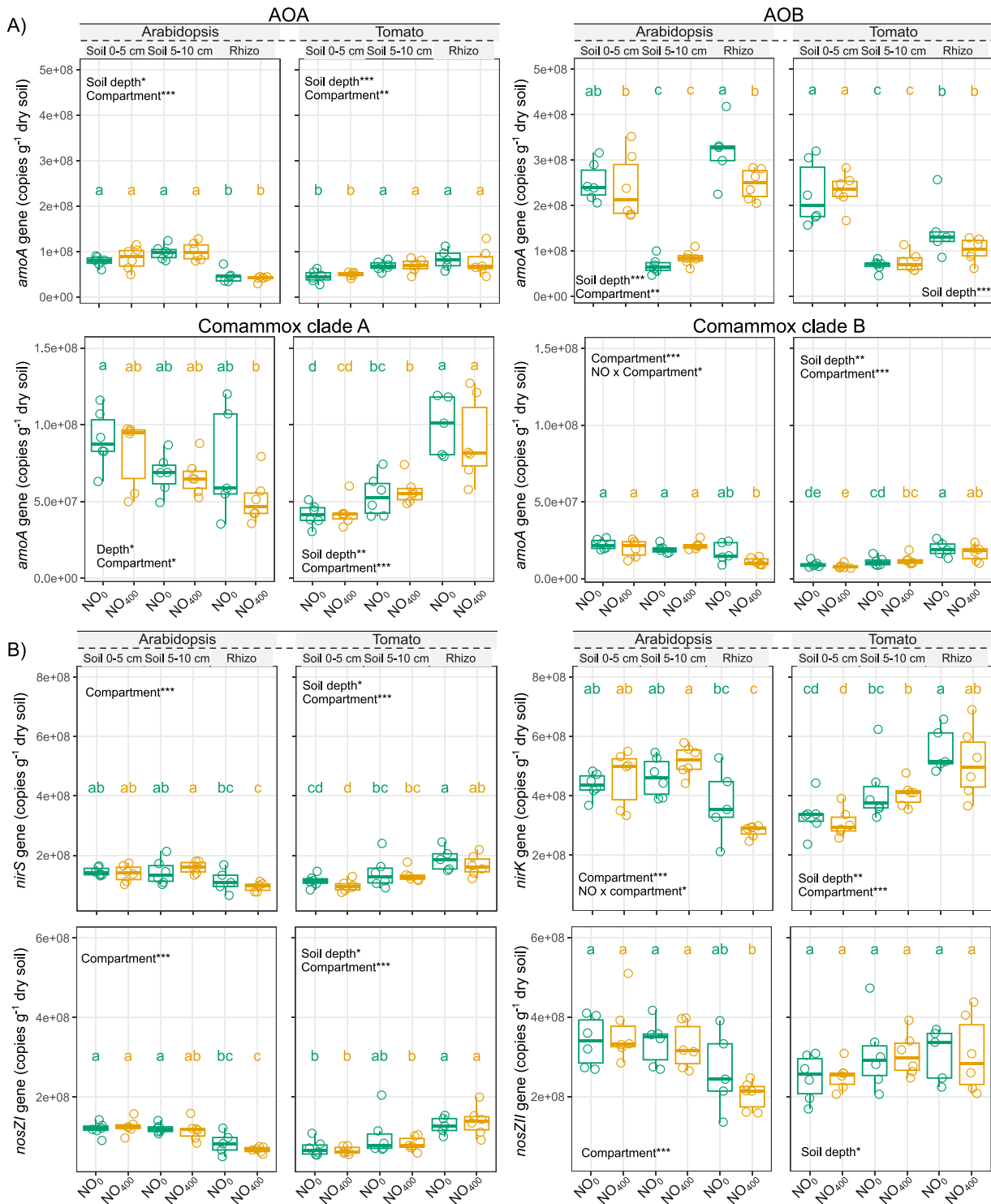


Figure 4. Boxplots showing the abundance of (A) ammonia oxidizers based on amoA gene copies of AOA, AOB, comammox clade A and comammox clade B, and the abundance of (B) denitrifiers based on nirS, nirK, nosZI, and nosZII gene copies, in bulk soil and the rhizosphere of Arabidopsis or tomato subjected to NO treatments (NO₀ and NO₄₀₀). For each box, the central horizontal line indicates the median, while the lower and upper edges represent the first and third quartiles, respectively. The whiskers extend to the minimum and maximum values, provided they do not exceed 1.5 times the interquartile range. Statistical tests are run independently for each experiment (Arabidopsis or tomato) and gene. Distinct letters above the boxes indicate significant differences based on non-parametric Kruskal-Wallis tests, followed by Fisher's least significant difference with Benjamini-Hochberg correction for pairwise comparisons ($P < .05$). Statistical significance for the effects of (i) NO, soil depth, and their interaction, and (ii) NO, compartment (bulk soil, rhizosphere and root), and their interaction, is indicated by asterisks in the figure (* $P < .05$, ** $P < .01$, *** $P < .001$), with ANOVA model outputs provided in Table S4.

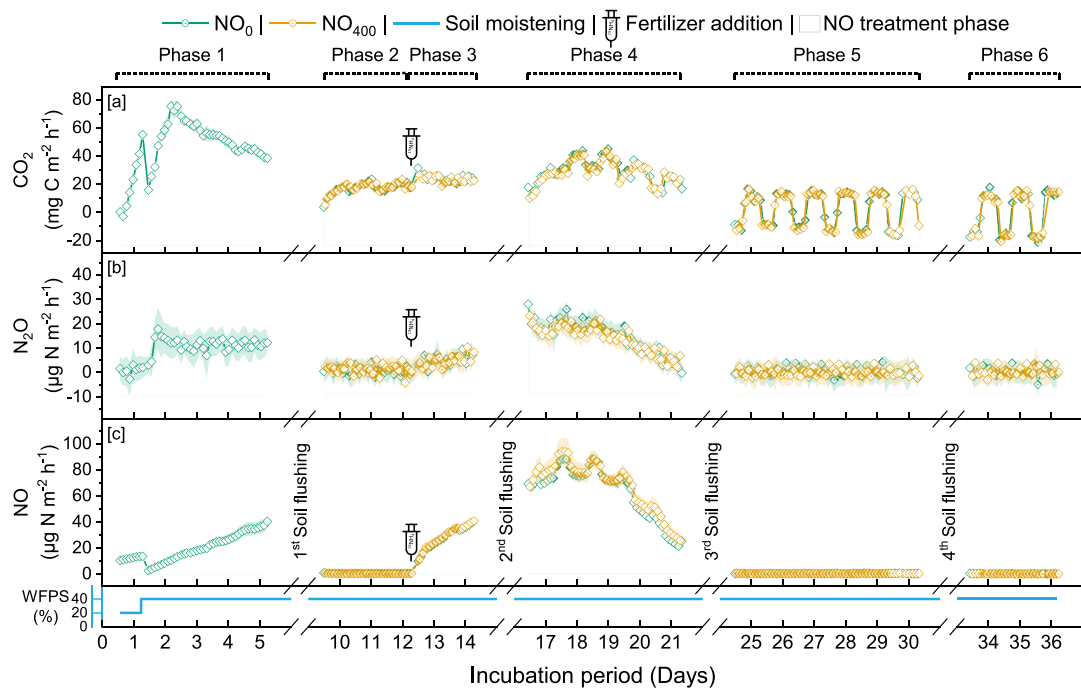


Figure 5. Soil fluxes of CO_2 , N_2O and NO from the *Arabidopsis* plant-soil experiment subjected to NO treatments (NO_0 and NO_{400}) over a 37-day incubation. Treatment phases, including ambient air, elevated NO (400 ppbv-NO), soil moistening, and fertilizer additions (using $(^{15}\text{NH}_4)_2\text{SO}_4$), are marked at the top, with NO treatment periods shaded in yellow. Intervals of interrupted surface flux measurements due to bottom-soil flushing, are indicated by dotted sections. Phases (P1-P6) are labelled to correspond with cumulative emissions reported in Table 1. Data are presented as mean \pm standard error (SE) across six replicates ($N=6$).

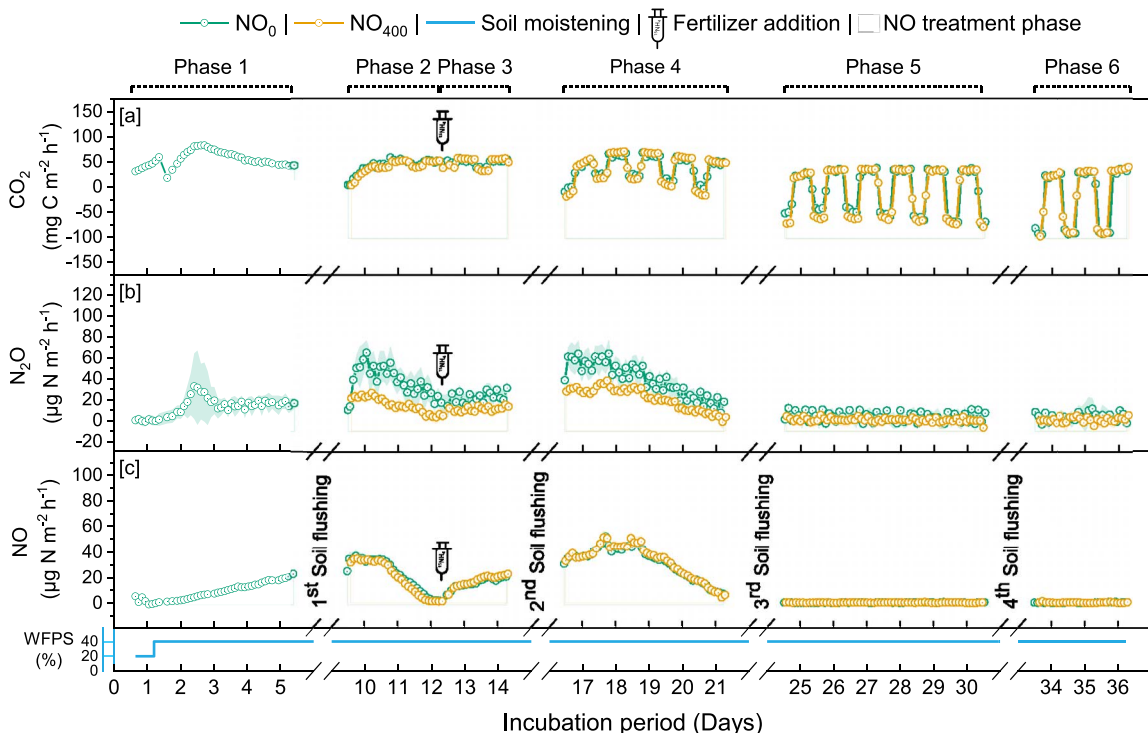


Figure 6. Soil fluxes of CO_2 , N_2O and NO from the tomato plant-soil experiment subjected to NO treatments (NO_0 and NO_{400}) over a 37-day incubation. Treatment phases, including ambient air, elevated NO (400 ppbv-NO), soil moistening, and fertilizer additions (using $(^{15}\text{NH}_4)_2\text{SO}_4$), are marked at the top, with NO treatment periods shaded in yellow. Intervals of interrupted surface flux measurements due to bottom-soil flushing, are indicated by dotted sections. Phases (P1-P6) are labelled to correspond with cumulative emissions reported in Table 1. Data are presented as mean \pm standard error (SE) across six replicates ($N=6$).

mycorrhizal fungi that form symbiotic associations with most terrestrial plants, including tomato [69].

Although the plant compartment exhibited the strongest effects, we found that exposure to NO, either alone or in

interaction with the plant compartment, also had a significant influence only on the diversity and the composition of the fungal community in the *Arabidopsis* experiment. The significant decrease in fungal diversity after NO_{400} exposure was

Table 1 Cumulative gas fluxes of carbon dioxide (CO₂), nitrous oxide (N₂O) and nitric oxide (NO) measured for both *Arabidopsis* and tomato experiments across the entire incubation period and individual phases (P1-P6). Data are presented as mean \pm standard error (SE) based on six replicates, with statistically significant differences indicated by asterisks (* $P < 0.05$, ** $P < 0.01$).

Gas species	Plant	Condition	Nitric oxide treatment	Phase 1 Days (0–6)	Phase 2 Days (10–12.5)	Phase 3 Days (12.5–15)	Phase 4 Days (17–22)	Phase 5 Days (25–31)	Phase 6 Days (34–37)	Σ Phase 1–6 Days (0–37)
CO₂ (mg C m⁻²)	<i>Arabidopsis</i>	Lights ON	NO ₀	2536 \pm 199	515 \pm 19	587 \pm 12**	1447 \pm 47*	-452 \pm 28	-375 \pm 23	4540 \pm 412*
		NO ₄₀₀	NO ₀	3410 \pm 179	474 \pm 28	476 \pm 24	1269 \pm 47	-517 \pm 85	-401 \pm 66	3556 \pm 206
		NO ₄₀₀	NO ₀	762 \pm 18	701 \pm 23*	568 \pm 9*	2035 \pm 46	841 \pm 20	359 \pm 7**	8147 \pm 322
		Total	NO ₀	5946 \pm 244	1215 \pm 21	630 \pm 11	2063 \pm 34	803 \pm 39	402 \pm 12	7836 \pm 137
		NO ₄₀₀	NO ₀	1236 \pm 15	1107 \pm 26	1155 \pm 19	3482 \pm 69	389 \pm 36	-16 \pm 29	12 687 \pm 384**
		Tomato	NO ₀	2190 \pm 89	1091 \pm 54*	927 \pm 77	1064 \pm 128*	3332 \pm 64	1 \pm 66	11 392 \pm 218
N₂O (μg N m⁻²)	<i>Arabidopsis</i>	Lights ON	NO ₄₀₀	943 \pm 49	871 \pm 38	604 \pm 84	3050 \pm 111*	-3398 \pm 293	-1474 \pm 612	-287 \pm 824
		Lights OFF	NO ₀	3058 \pm 89	1846 \pm 59	1336 \pm 33	1351 \pm 37	1956 \pm 66	846 \pm 103	12 220 \pm 188
		NO ₄₀₀	NO ₀	5248 \pm 107	1759 \pm 54	2263 \pm 79	3556 \pm 79	1870 \pm 169	710 \pm 83	12 387 \pm 236
		Total	NO ₀	2937 \pm 55*	2701 \pm 90	2222 \pm 66	4159 \pm 125	-977 \pm 225	-1531 \pm 221	12 226 \pm 360
		NO ₄₀₀	NO ₀	494 \pm 36	34 \pm 35	103 \pm 16	952 \pm 55*	-1528 \pm 283	-764 \pm 602	12 100 \pm 959
		Lights ON	NO ₀	56 \pm 18	85 \pm 24	85 \pm 24	825 \pm 47	4 \pm 18	15 \pm 20	1564 \pm 116
NO (μg N m⁻²)	<i>Arabidopsis</i>	Lights ON	NO ₀	619 \pm 55	24 \pm 16	132 \pm 20	863 \pm 64	47 \pm 16	0 \pm 5	1539 \pm 103
		Lights OFF	NO ₀	58 \pm 13	143 \pm 7	836 \pm 31	-9 \pm 41	10 \pm 20	1583 \pm 146	
		NO ₄₀₀	NO ₀	1113 \pm 88	58 \pm 33	235 \pm 33	1815 \pm 106*	50 \pm 23	14 \pm 21	1758 \pm 68
		NO ₄₀₀	NO ₀	114 \pm 24	228 \pm 19	1661 \pm 46	15 \pm 69	29 \pm 24	3147 \pm 249	
		Total	NO ₀	1113 \pm 270	466 \pm 123*	2411 \pm 416*	312 \pm 64**	165 \pm 86	3297 \pm 150	
		Tomato	NO ₄₀₀	978 \pm 422	528 \pm 16	256 \pm 25	1316 \pm 43	113 \pm 35	21 \pm 38	5900 \pm 1026*
NO₂ (μg N m⁻²)	<i>Arabidopsis</i>	Lights ON	NO ₀	860 \pm 137	1547 \pm 486*	605 \pm 142*	2295 \pm 420*	290 \pm 139	167 \pm 121	5660 \pm 642**
		NO ₄₀₀	NO ₀	1838 \pm 95	566 \pm 26	298 \pm 17	1253 \pm 87	99 \pm 26	34 \pm 48	3180 \pm 301
		Total	NO ₀	2660 \pm 752*	1072 \pm 63	4706 \pm 835*	622 \pm 200*	323 \pm 197	11 559 \pm 1674**	
		NO ₄₀₀	NO ₀	1094 \pm 39	553 \pm 24	2570 \pm 120	201 \pm 60	65 \pm 90	6089 \pm 653	
		Lights OFF	NO ₀	928 \pm 78	22 \pm 2	572 \pm 14*	3906 \pm 218	34 \pm 1	13 \pm 1	5565 \pm 210
		NO ₄₀₀	NO ₀	1322 \pm 85	23 \pm 1	489 \pm 21	3862 \pm 364	36 \pm 2	13 \pm 2	5259 \pm 547
NO_x (μg N m⁻²)	<i>Arabidopsis</i>	Lights ON	NO ₀	2250 \pm 160	42 \pm 4	777 \pm 65	3756 \pm 192	30 \pm 1	8 \pm 2	5912 \pm 210
		Lights OFF	NO ₀	942 \pm 95	1384 \pm 118	888 \pm 62	4181 \pm 448	33 \pm 2	9 \pm 1	6420 \pm 698
		Total	NO ₀	801 \pm 71	1384 \pm 125	801 \pm 71	3880 \pm 371	73 \pm 6	47 \pm 37	11 477 \pm 410
		NO ₄₀₀	NO ₀	664 \pm 59	777 \pm 65	462 \pm 40	1988 \pm 194	33 \pm 4	22 \pm 2	11 680 \pm 1245
		Lights ON	NO ₀	706 \pm 2	3979 \pm 118	748 \pm 32	3790 \pm 118	72 \pm 6	3380 \pm 116	
		Total	NO ₀	7038 \pm 151	7038 \pm 282	7038 \pm 151	7038 \pm 898	7570 \pm 898	7570 \pm 898	3473 \pm 343

Table 2. Impact of exogenous NO on the N balance. ^{15}N recovery percentages in both *Arabidopsis* and tomato experiments, showing nitrate (NO_3^-), dissolved organic nitrogen (DON), microbial biomass nitrogen (MBN) and total nitrogen (TN) across two soil depth segments (0–5 cm and 5–10 cm), as well as cumulative depth, under varying NO treatments. In the *Arabidopsis* experiment, the soil was labelled with $(^{15}\text{NH}_4)_2\text{SO}_4$ at a 30% atom ^{15}N enrichment, while in the tomato experiment, the soil was labelled with $(^{15}\text{NH}_4)_2\text{SO}_4$ at a 70% atom ^{15}N enrichment, and both were applied at a rate of 60 kg N ha $^{-1}$. Values are reported as mean \pm standard error (SE) from six replicates, with statistically significant differences denoted by asterisks (* $P < .05$).

	Plants	Nitric oxide treatment	^{15}N Recovery % (0–5 cm)	^{15}N Recovery % (5–10 cm)	^{15}N Recovery % Total
NO_3^-	<i>Arabidopsis</i>	NO_0	45 \pm 1	19 \pm 1	63 \pm 1*
		NO_{400}	36 \pm 5	18 \pm 1	48 \pm 7
	<i>Tomato</i>	NO_0	17 \pm 1*	8 \pm 1*	24 \pm 2
		NO_{400}	14 \pm 1	11 \pm 1	24 \pm 1
DON	<i>Arabidopsis</i>	NO_0	6 \pm 1	3 \pm 0	8 \pm 1
		NO_{400}	14 \pm 6	2 \pm 0	16 \pm 6
	<i>Tomato</i>	NO_0	1 \pm 0	0 \pm 0	2 \pm 0
		NO_{400}	2 \pm 0	1 \pm 0	2 \pm 0
MBN	<i>Arabidopsis</i>	NO_0	13 \pm 3*	8 \pm 1	24 \pm 3
		NO_{400}	23 \pm 3	7 \pm 2	30 \pm 4
	<i>Tomato</i>	NO_0	2 \pm 1	2 \pm 1	4 \pm 1
		NO_{400}	2 \pm 0	2 \pm 1	5 \pm 1
TN	<i>Arabidopsis</i>	NO_0	59 \pm 3	19 \pm 1	78 \pm 4
		NO_{400}	54 \pm 5	18 \pm 1	72 \pm 6
	<i>Tomato</i>	NO_0	24 \pm 1*	11 \pm 1	35 \pm 0
		NO_{400}	21 \pm 1	12 \pm 1	33 \pm 2

concomitant with lower inorganic N pools, which may reflect the potential roles of fungi in organic matter decomposition and N turnover [70]. Since changes in NO homeostasis in *Arabidopsis* can affect microbial communities [66], this fungal response may have been indirectly mediated by NO-induced alterations in *Arabidopsis* physiology, even though this effect of NO was observed in the bulk soil. Thus, comparison of microbial communities between bulk (i.e. non-rhizospheric) and non-planted soils revealed significant effects of plants also in the bulk soil [71]. Accordingly, Schulz-Bohm et al. [72] showed that soil microorganisms can respond over long distances to volatile organic compounds emitted by plants, especially under stress. It is therefore not possible to decipher the mechanism by which NO influenced the fungal community, as it plays significant roles in various processes not only in plants but also across multiple fungal species, including spore formation, nitrogen metabolism, virulence and pathogenicity, stress tolerance capacity and hyphal extension [14, 73–76]. For example, NO can affect the balance between conidiation and sexual reproduction with higher NO levels both reducing conidiation and promoting cleistothecial formation in *Aspergillus* [75, 77]. Exogenous NO has been also associated with mycotoxin production in *Aspergillus* [75] and is related to plant infection in other fungal taxa such as *Botrytis* [76], *Blumeria* [78] or *Fusarium* [79]. While NO is known to have bactericidal effects through both oxidative and nitrosative stressors [15, 80], no significant effects of NO_{400} were observed on the diversity and composition of the bacterial community as previously observed in non-planted soil [16]. This could be due to the fact that bacteriostasis is the dominant manifestation of NO toxicity against most bacteria [81]. Alternatively, the NO concentration used in our experiment could have been too low to be toxic or that toxicity was limited to certain bacterial taxa, making such effect undetectable at the community level. Because of methodological constraints associated with the dynamic manipulation of NO concentrations, studies addressing the role of NO in soil communities or in association with plant

roots are still scarce [16, 82]. Our study advances this field by applying an innovative mesocosm system to investigate how environmentally realistic NO concentrations shape bacterial and fungal communities in plant roots or in the rhizosphere.

Monitoring CO_2 emissions revealed that the cumulative fluxes were negatively affected in the *Arabidopsis* experiment, whereas a significant decrease in total CO_2 fluxes was observed only during phase 2 in the tomato experiment. The significant decrease in CO_2 fluxes under elevated NO only during the photoperiod suggests a positive effect on photosynthesis with increased CO_2 assimilation. In contrast, previous studies observed that exposure of lettuce to high NO concentration caused an inhibition of the net assimilation of CO_2 due to a direct effect on photosynthesis rather than a change in stomatal conductance, and it did not affect respiration [83, 84]. However, in our study, the lower CO_2 fluxes with the light on, and higher fluxes with the light off, could be attributed to an overall increase in photosynthetic and respiratory activities due to the larger leaf area of *Arabidopsis* plants under NO_{400} treatment.

To further explore the impact of exogenous NO, we focused on N-cycling and quantified inorganic N-pools, N balance, N_2O and NO emissions as well as the abundance of ammonia-oxidizers and denitrifiers. Along with lower ^{15}N recovery of the labelled NH_4^+ as NO_3^- under NO_{400} in the *Arabidopsis* experiment, we found lower abundances of AOB in the rhizosphere. This suggests a detrimental effect of NO_{400} on the nitrification process, which consists in the oxidation of NH_4^+ to NO_3^- to generate energy for microbial growth. This decrease in the abundance of AOB, together with the reduced ^{15}N recovery as NO_3^- , could partly explain the lower N_2O fluxes observed under NO_{400} in the *Arabidopsis* experiment. Additionally, this detrimental effect on nitrifiers could further limit NO_3^- availability as a substrate for denitrification, ultimately leading to reduced N_2O emissions by denitrifiers. Since greater ammonium uptake by the microbial biomass was observed in the *Arabidopsis* experiment under NO_{400} , this lower abundance of AOB may be due to increased competition for ammonium

between assimilatory and dissimilatory microbial processes after exposure to NO_{400} . Although earlier studies showed that the uptake of N by European beech roots increased significantly with elevated NO concentrations [85], the N-content in tomato plants was unaffected by NO_{400} . This discrepancy can be explained by the fact that the NO effects on N uptake depend on soil N availability, with stronger effects observed under higher N availability [86]. Similarly, neither the abundance of N-cycling communities, N pools in soil, or analyzed plant transcripts showed clear trends in response to NO_{400} in the tomato experiment. As such, the observed reduction of up to 59% in N_2O fluxes—associated only with a slight increase in belowground biomass but not plant N content—remains unexplained and warrants further investigation. Previous studies showed that plant photosynthesis reduced N_2O emission from plant-soil systems, without providing insight into the underlying mechanisms [87].

In conclusion, our experiments using an innovative plant-soil mesocosm system that dynamically changes background NO concentrations highlight that exogenous NO in soil can alter *Arabidopsis* physiology, accompanied by shifts in the fungal community and nitrogen cycling. Specifically, exposure to NO_{400} increased leaf area while reducing the abundance of certain N-cycling communities, ^{15}N recovery as NO_3^- , and cumulative CO_2 fluxes. Although most plant and microbial parameters remained unaffected in the tomato experiment, the substantial decrease in N_2O emissions following NO flushing is particularly intriguing, as it was not associated with detectable changes in microbial community composition, N pools, or the expression levels of the studied plant transcripts. Although the duration of the NO treatment in our experiment reflects continuous field NO measurements, potential long-term ecological effects may have been overlooked. Overall, our work opens intriguing perspectives on the potential contribution of exogenous NO to plant-microbe interactions but its broader impact on soil ecosystems appears limited and warrants further investigation through long-term experiments.

Author contributions

E.P.-V., D.W., N.B., K.B.-B., M.D. and L.P. (Conceptualization), L.S., E.P.-V., A.B., P.T., P.L., M.-C.B., F.E., and D.B. (Methodology), E.P.-V., L.S., A.B., P.T., P.L., M.-C.B. and D.B. (Data analysis), E.P.-V. and L.P. (Writing—original draft), all. (Writing—review and editing), D.W., N.B., K.B.-B., M.D. and L.P. (Supervision), D.W., N.B., K.B.-B., M.D. and L.P. (Funding acquisition)

Supplementary material

Supplementary material is available at ISME Communications online.

Conflicts of interest

None declared.

Funding

This work was co-funded by the French ANR and German DFG under contract number ANR-20-CE92-0004, DFG BU 1173/25-1 and DFG BR 2265/5-1.

Data availability

Raw sequence data of 16S rRNA and fungal ITS have been deposited in the Sequence Read Archive NCBI under Bio-Project accession numbers PRJNA1172607 and PRJNA1172642, respectively.

References

- Medinets S, Skiba U, Rennenberg H. et al. A review of soil NO transformation: associated processes and possible physiological significance on organisms. *Soil Biol Biochem* 2015;80:92–117. <https://doi.org/10.1016/j.soilbio.2014.09.025>
- Fowler D, Pilegaard K, Sutton MA. et al. Atmospheric composition change: ecosystems-atmosphere interactions. *Atmos Environ* 2009;43:5193–267. <https://doi.org/10.1016/j.atmosenv.2009.07.068>
- Butterbach-Bahl K, Kahl M, Mykhayliv L. et al. A European-wide inventory of soil NO emissions using the biogeochemical models DNDC/Forest-DNDC. *Atmos Environ* 2009;43:1392–402. <https://doi.org/10.1016/j.atmosenv.2008.02.008>
- Heil J, Vereecken H, Brüggemann N. A review of chemical reactions of nitrification intermediates and their role in nitrogen cycling and nitrogen trace gas formation in soil. *Eur J Soil Sci* 2016;67:23–39. <https://doi.org/10.1111/ejss.12306>
- Astier J, Gross I, Durner J. Nitric oxide production in plants: an update. *J Exp Bot* 2018;69:3401–11. <https://doi.org/10.1093/jxb/erx420>
- Welle M, Niether W, Stöhr C. The underestimated role of plant root nitric oxide emission under low-oxygen stress. *Front Plant Sci* 2024;15:1290700. <https://doi.org/10.3389/fpls.2024.1290700>
- Pilegaard K. Processes regulating nitric oxide emissions from soils. *Philos Trans R Soc B Biol Sci* 2013;368:20130126. <https://doi.org/10.1098/rstb.2013.0126>
- Medinets S, Gasche R, Kiese R. et al. Seasonal dynamics and profiles of soil NO concentrations in a temperate forest. *Plant Soil* 2019;445:335–48. <https://doi.org/10.1007/s11104-019-04305-5>
- Gut A, van Dijk SM, Scheibe M. et al. NO emission from an Amazonian rain forest soil: continuous measurements of NO flux and soil concentration. *J Geophys Res-Atmos* 2002;107:8057. <https://doi.org/10.1029/2001JD000521>
- Ma M, Wendehenne D, Philippot L. et al. Physiological significance of pedospheric nitric oxide for root growth, development and organismic interactions. *Plant Cell Environ* 2020;43:2336–54. <https://doi.org/10.1111/pce.13850>
- Spiro S. Regulators of bacterial responses to nitric oxide. *FEMS Microbiol Rev* 2007;31:193–211. <https://doi.org/10.1111/j.1574-6976.2006.00061.x>
- Gusarov I, Shatalin K, Starodubtseva M. et al. Endogenous nitric oxide protects bacteria against a wide spectrum of antibiotics. *Science* 2009;325:1380–4. <https://doi.org/10.1126/science.1175439>
- Arruebarrena Di Palma A, Pereyra CM, Moreno Ramirez L. et al. Denitrification-derived nitric oxide modulates biofilm formation in *Azospirillum brasiliense*. *FEMS Microbiol Lett* 2013;338:77–85. <https://doi.org/10.1111/1574-6968.12030>
- Cánovas D, Marcos JF, Marcos AT. et al. Nitric oxide in fungi: is there NO light at the end of the tunnel? *Curr Genet* 2016;62:513–8. <https://doi.org/10.1007/s00294-016-0574-6>
- Privett BJ, Broadnax AD, Bauman SJ. et al. Examination of bacterial resistance to exogenous nitric oxide. *Nitric Oxide* 2012;26:169–73. <https://doi.org/10.1016/j.niox.2012.02.002>
- Subramaniam L, Pérez-Valera E, Berger A. et al. The role of different exogenous NO concentrations on C and N biogeochemistry

of an agricultural soil. *Biogeochemistry* 2025; **168**:58. <https://doi.org/10.1007/s10533-025-01248-1>

17. Klessig DF, Durner J, Noad R. et al. Nitric oxide and salicylic acid signaling in plant defense. *Proc Natl Acad Sci* 2000; **97**:8849–55. <https://doi.org/10.1073/pnas.97.16.8849>

18. Leitner M, Vandelle E, Gaupels F. et al. NO signals in the haze: nitric oxide signalling in plant defence. *Curr Opin Plant Biol* 2009; **12**:451–8. <https://doi.org/10.1016/j.pbi.2009.05.012>

19. Gayatri G, Agurla S, Raghavendra AS. Nitric oxide in guard cells as an important secondary messenger during stomatal closure. *Front Plant Sci* 2013; **4**:1–11. <https://doi.org/10.3389/fpls.2013.00425>

20. Wendehenne D, Gao Q, Kachroo A. et al. Free radical-mediated systemic immunity in plants. *Curr Opin Plant Biol* 2014; **20**:127–34. <https://doi.org/10.1016/j.pbi.2014.05.012>

21. Wang P, Du Y, Hou Y-J. et al. Nitric oxide negatively regulates abscisic acid signaling in guard cells by S-nitrosylation of OST1. *Proc Natl Acad Sci* 2015; **112**:613–8. <https://doi.org/10.1073/pnas.1423481112>

22. Sun LR, Yue CM, Hao FS. Update on roles of nitric oxide in regulating stomatal closure. *Plant Signal Behav* 2019; **14**:e1649569. <https://doi.org/10.1080/15592324.2019.1649569>

23. Sanchez-Corriónero A, Sánchez-Vicente I, Arteaga N. et al. Fine-tuned nitric oxide and hormone interface in plant root development and regeneration. *J Exp Bot* 2023; **74**:6104–18. <https://doi.org/10.1093/jxb/erac508>

24. Besson-Bard A, Pugin A, Wendehenne D. New insights into nitric oxide Signaling in plants. *Annu Rev Plant Biol* 2008; **59**:21–39. <https://doi.org/10.1146/annurev.arplant.59.032607.092830>

25. Subramaniam L, Engelsberger F, Wolf B. et al. An innovative soil mesocosm system for studying the effect of soil moisture and background NO on soil surface C and N trace gas fluxes. *Biol Fertil Soils* 2024; **60**:1143–57. <https://doi.org/10.1007/s00374-024-01862-5>

26. Ganger MT, Dietz GD, Ewing SJ. A common base method for analysis of qPCR data and the application of simple blocking in qPCR experiments. *BMC Bioinformatics* 2017; **18**:534. <https://doi.org/10.1186/s12859-017-1949-5>

27. Czechowski T, Stitt M, Altmann T. et al. Genome-wide identification and testing of superior reference genes for transcript normalization in *Arabidopsis*. *Plant Physiol* 2005; **139**:5–17. <https://doi.org/10.1104/pp.105.063743>

28. Hussain A, Yun B-W, Kim JH. et al. Novel and conserved functions of S-nitrosoglutathione reductase in tomato. *J Exp Bot* 2019; **70**:4877–86. <https://doi.org/10.1093/jxb/erz234>

29. Expósito-Rodríguez M, Borges AA, Borges-Pérez A. et al. Selection of internal control genes for quantitative real-time RT-PCR studies during tomato development process. *BMC Plant Biol* 2008; **8**:131. <https://doi.org/10.1186/1471-2229-8-131>

30. Romdhane S, Spor A, Aubert J. et al. Unraveling negative biotic interactions determining soil microbial community assembly and functioning. *ISME J* 2022; **16**:296–306. <https://doi.org/10.1038/s41396-021-01076-9>

31. Edgar RC. Search and clustering orders of magnitude faster than BLAST. *Bioinformatics* 2010; **26**:2460–1. <https://doi.org/10.1093/bioinformatics/btq461>

32. Quast C, Pruesse E, Yilmaz P. et al. The SILVA ribosomal RNA gene database project: improved data processing and web-based tools. *Nucleic Acids Res* 2013; **41**:D590–6. <https://doi.org/10.1093/nar/gks1219>

33. Altschul SF, Gish W, Miller W. et al. Basic local alignment search tool. *J Mol Biol* 1990; **215**:403–10. [https://doi.org/10.1016/S0022-2836\(05\)80360-2](https://doi.org/10.1016/S0022-2836(05)80360-2)

34. Nilsson RH, Larsson K-H, Taylor AFS. et al. The UNITE database for molecular identification of fungi: handling dark taxa and parallel taxonomic classifications. *Nucleic Acids Res* 2019; **47**:D259–64. <https://doi.org/10.1093/nar/gky1022>

35. Meyer C, Jeanbille M, Breuil M-C. et al. Dynamic response of soil microbial communities and network to hymexazol exposure. *Sci Total Environ* 2024; **957**:177557. <https://doi.org/10.1016/j.scitotenv.2024.177557>

36. Bintarti AF, Kost E, Kundel D. et al. Cropping system modulates the effect of spring drought on ammonia-oxidizing communities. *Soil Biol Biochem* 2025; **201**:109658. <https://doi.org/10.1016/j.soilbio.2024.109658>

37. Domeignoz-Horta LA, Philippot L, Peyraud C. et al. Peaks of in situ N₂O emissions are influenced by N₂O-producing and reducing microbial communities across arable soils. *Glob Chang Biol* 2018; **24**:360–70. <https://doi.org/10.1111/gcb.13853>

38. Dannenmann M, Simon J, Gasche R. et al. Tree girdling provides insight on the role of labile carbon in nitrogen partitioning between soil microorganisms and adult European beech. *Soil Biol Biochem* 2009; **41**:1622–31. <https://doi.org/10.1016/j.soilbio.2009.04.024>

39. Dannenmann M, Díaz-Pinés E, Kitzler B. et al. Postfire nitrogen balance of Mediterranean shrublands: direct combustion losses versus gaseous and leaching losses from the postfire soil mineral nitrogen flush. *Glob Chang Biol* 2018; **24**:4505–20. <https://doi.org/10.1111/gcb.14388>

40. Dannenmann M, Bimüller C, Gschwendtner S. et al. Climate change impairs nitrogen cycling in European beech forests. *PLoS One* 2016; **11**:e0158823. <https://doi.org/10.1371/journal.pone.0158823>

41. R Core Team. R: A Language and Environment for Statistical Computing. Vienna, Austria: R Foundation for Statistical Computing, 2025.

42. Liu C, Cui Y, Li X. et al. Microeco: an R package for data mining in microbial community ecology. *FEMS Microbiol Ecol* 2021; **97**:fiaa255. <https://doi.org/10.1093/femsec/fiaa255>

43. McMurdie PJ, Holmes S. Phyloseq: an R package for reproducible interactive analysis and graphics of microbiome census data. *PLoS One* 2013; **8**:e61217. <https://doi.org/10.1371/journal.pone.0061217>

44. Oksanen J, Simpson GL, Blanchet FG. et al. Vegan: Community Ecology Package. Package version: 2.7-2, 2024.

45. Martinez Arbizu P. pairwiseAdonis: pairwise multilevel comparison using Adonis. R Package Version 04 2020. Available from: <https://github.com/pmartinezarbizu/pairwiseAdonis>.

46. Huang X, Stettmaier K, Michel C. et al. Nitric oxide is induced by wounding and influences jasmonic acid signaling in *Arabidopsis thaliana*. *Planta* 2004; **218**:938–46. <https://doi.org/10.1007/s00425-003-1178-1>

47. Lindermayr C, Saalbach G, Durner J. Proteomic identification of S-Nitrosylated proteins in *Arabidopsis*. *Plant Physiol* 2005; **137**:921–30. <https://doi.org/10.1104/pp.104.058719>

48. Grün S, Lindermayr C, Sell S. et al. Nitric oxide and gene regulation in plants. *J Exp Bot* 2006; **57**:507–16. <https://doi.org/10.1093/jxb/erj053>

49. Palmieri MC, Sell S, Huang X. et al. Nitric oxide-responsive genes and promoters in *Arabidopsis thaliana*: a bioinformatics approach. *J Exp Bot* 2008; **59**:177–86. <https://doi.org/10.1093/jxb/erm345>

50. Melo NKG, Bianchetti RE, Lira BS. et al. Nitric oxide, ethylene, and auxin cross talk mediates greening and plastid development in Deetiolating tomato seedlings. *Plant Physiol* 2016; **170**:2278–94. <https://doi.org/10.1104/pp.16.00023>

51. León J, Costa Á, Castillo M-C. Nitric oxide triggers a transient metabolic reprogramming in *Arabidopsis*. *Sci Rep* 2016;6:37945. <https://doi.org/10.1038/srep37945>

52. Frungillo L, Skelly MJ, Loake GJ. et al. S-nitrosothiols regulate nitric oxide production and storage in plants through the nitrogen assimilation pathway. *Nat Commun* 2014;5:5401. <https://doi.org/10.1038/ncomms6401>

53. Kasten D, Durner J, Gaupels F. Gas alert: the NO₂ pitfall during NO fumigation of plants. *Front Plant Sci* 2017;8:85. <https://doi.org/10.3389/fpls.2017.00085>

54. Nelson BS, Bryant DJ, Alam MS. et al. Extreme concentrations of nitric oxide control daytime oxidation and quench nocturnal oxidation chemistry in Delhi during highly polluted episodes. *Environ Sci Technol Lett* 2023;10:520–7. <https://doi.org/10.1021/acs.estlett.3c00171>

55. Durner J, Wendehenne D, Klessig DF. Defense gene induction in tobacco by nitric oxide, cyclic GMP, and cyclic ADP-ribose. *Proc Natl Acad Sci* 1998;95:10328–33. <https://doi.org/10.1073/pnas.95.17.10328>

56. Mira MM, Wally OSD, Elhiti M. et al. Jasmonic acid is a downstream component in the modulation of somatic embryogenesis by *Arabidopsis* class 2 phytoglobin. *J Exp Bot* 2016;67:2231–46. <https://doi.org/10.1093/jxb/erw022>

57. Pescador L, Fernandez I, Pozo MJ. et al. Nitric oxide signalling in roots is required for MYB72-dependent systemic resistance induced by *Trichoderma* volatile compounds in *Arabidopsis*. *J Exp Bot* 2022;73:584–95. <https://doi.org/10.1093/jxb/erab294>

58. Leshem YY, Haramaty E. The characterization and contrasting effects of the nitric oxide free radical in vegetative stress and senescence of *Pisum sativum* Linn. *Foliage J Plant Physiol* 1996;148: 258–63. [https://doi.org/10.1016/S0176-1617\(96\)80251-3](https://doi.org/10.1016/S0176-1617(96)80251-3)

59. Turner TR, James EK, Poole PS. The plant microbiome. *Genome Biol* 2013;14:209. <https://doi.org/10.1186/gb-2013-14-6-209>

60. Trivedi P, Leach JE, Tringe SG. et al. Plant-microbiome interactions: from community assembly to plant health. *Nat Rev Microbiol* 2020;18:607–21. <https://doi.org/10.1038/s41579-020-0412-1>

61. Philippot L, Raaijmakers JM, Lemanceau P. et al. Going back to the roots: the microbial ecology of the rhizosphere. *Nat Rev Microbiol* 2013;11:789–99. <https://doi.org/10.1038/nrmicro3109>

62. Fierer N. Embracing the unknown: disentangling the complexities of the soil microbiome. *Nat Rev Microbiol* 2017;15:579–90. <https://doi.org/10.1038/nrmicro.2017.87>

63. Berg G, Smalla K. Plant species and soil type cooperatively shape the structure and function of microbial communities in the rhizosphere. *FEMS Microbiol Ecol* 2009;68:650610. <https://doi.org/10.1111/j.1574-6941.2009.00654.x>

64. Lundberg DS, Lebeis SL, Paredes SH. et al. Defining the core *Arabidopsis thaliana* root microbiome. *Nature* 2012;488:86–90. <https://doi.org/10.1038/nature11237>

65. Tian B, Zhang C, Ye Y. et al. Beneficial traits of bacterial endophytes belonging to the core communities of the tomato root microbiome. *Agric Ecosyst Environ* 2017;247:149–56. <https://doi.org/10.1016/j.agee.2017.06.041>

66. Berger A, Pérez-Valera E, Blouin M. et al. Microbiota responses to mutations affecting NO homeostasis in *Arabidopsis thaliana*. *New Phytol* 2024;244:2008–23. <https://doi.org/10.1111/nph.20159>

67. Bulgarelli D, Rott M, Schlaepi K. et al. Revealing structure and assembly cues for *Arabidopsis* root-inhabiting bacterial microbiota. *Nature* 2012;488:91–5. <https://doi.org/10.1038/nature11336>

68. Delaux P-M, Varala K, Edger PP. et al. Comparative Phylogenomics uncovers the impact of symbiotic associations on host genome evolution. *PLoS Genet* 2014;10:e1004487. <https://doi.org/10.1371/journal.pgen.1004487>

69. Bonfante P, Genre A. Mechanisms underlying beneficial plant-fungus interactions in mycorrhizal symbiosis. *Nat Commun* 2010;1:48. <https://doi.org/10.1038/ncomms1046>

70. Treseder KK, Lennon JT. Fungal traits that drive ecosystem dynamics on land. *Microbiol Mol Biol Rev* 2015;79:243–62. <https://doi.org/10.1128/MMBR.00001-15>

71. Blouin M, Jacquiod S. Sampling the control bulk soil for rhizosphere and drilosphere microbial studies. *Geoderma* 2020;380:114674. <https://doi.org/10.1016/j.geoderma.2020.114674>

72. Schulz-Bohm K, Gerards S, Hundscheid M. et al. Calling from distance: attraction of soil bacteria by plant root volatiles. *ISME J* 2018;12:1252–62. <https://doi.org/10.1038/s41396-017-0035-3>

73. Zhao Y, Lim J, Xu J. et al. Nitric oxide as a developmental and metabolic signal in filamentous fungi. *Mol Microbiol* 2020;113: 872–82. <https://doi.org/10.1111/mmi.14465>

74. Kong W, Huang C, Chen Q. et al. Nitric oxide alleviates heat stress-induced oxidative damage in *Pleurotus eryngii* var. *tuoliensis*. *Fungal Genet Biol* 2012;49:15–20. <https://doi.org/10.1016/j.fgb.2011.12.003>

75. Baidya S, Cary JW, Grayburn WS. et al. Role of nitric oxide and Flavohemoglobin homolog genes in *Aspergillus nidulans* sexual development and mycotoxin production. *Appl Environ Microbiol* 2011;77:5524–28. <https://doi.org/10.1128/AEM.00638-11>

76. Turrión-Gómez JL, Benito EP. Flux of nitric oxide between the necrotrophic pathogen *Botrytis cinerea* and the host plant. *Mol Plant Pathol* 2011;12:606–16. <https://doi.org/10.1111/j.1364-3703.2010.00695.x>

77. Marcos AT, Ramos MS, Marcos JF. et al. Nitric oxide synthesis by nitrate reductase is regulated during development in *Aspergillus*. *Mol Microbiol* 2016;99:15–33. <https://doi.org/10.1111/mmi.13211>

78. Prats E, Carver TLW, Mur LAJ. Pathogen-derived nitric oxide influences formation of the appressorium infection structure in the phytopathogenic fungus *Blumeria graminis*. *Res Microbiol* 2008;159:476–80. <https://doi.org/10.1016/j.resmic.2008.04.001>

79. Ding Y, Gardiner DM, Xiao D. et al. Regulators of nitric oxide signaling triggered by host perception in a plant pathogen. *Proc Natl Acad Sci* 2020;117:11147–57. <https://doi.org/10.1073/pnas.1918977117>

80. Hetrick EM, Shin JH, Stasko NA. et al. Bactericidal efficacy of nitric oxide-releasing silica nanoparticles. *ACS Nano* 2008;2: 235–46. <https://doi.org/10.1021/nn700191f>

81. Jones-Carson J, Yahashiri A, Kim J-S. et al. Nitric oxide disrupts bacterial cytokinesis by poisoning purine metabolism. *Sci Adv* 2020;6:eaaz0260. <https://doi.org/10.1126/sciadv.aaz0260>

82. Garrido-Amador P, Stortenbeker N, Wessels HJCT. et al. Enrichment and characterization of a nitric oxide-reducing microbial community in a continuous bioreactor. *Nat Microbiol* 2023;8: 1574–86. <https://doi.org/10.1038/s41564-023-01425-8>

83. Saxe H. Effects of NO, NO₂ and CO₂ on net photosynthesis, dark respiration and transpiration of pot plants. *New Phytol* 1986;103: 185–97. <https://doi.org/10.1111/j.1469-8137.1986.tb00607.x>

84. Caporn SJM, Mansfield TA, Hand DW. Low temperature-enhanced inhibition of photosynthesis by oxides of nitrogen in lettuce (*Lactuca sativa* L.). *New Phytol* 1991;118:309–13. <https://doi.org/10.1111/j.1469-8137.1991.tb00982.x>

85. Simon J, Stoelken G, Rienks M. et al. Rhizospheric NO interacts with the acquisition of reduced N sources by the roots of European beech (*Fagus sylvatica* L.). *FEBS Lett* 2009;583:2907–10. <https://doi.org/10.1016/j.febslet.2009.07.052>

86. Simon J, Dong F, Buegger F. et al. Rhizospheric NO affects N uptake and metabolism in scots pine (*Pinus sylvestris* L.) seedlings depending on soil N availability and N source. *Plant Cell Environ* 2013;36:1019–26. <https://doi.org/10.1111/pce.12034>

87. Schützenmeister K, Meurer KHE, Gronwald M. et al. N₂O emissions from plants are reduced under photosynthetic activity. *Plant-Environ Interact* 2020;1:48–56. <https://doi.org/10.1002/pei3.10015>